HOSTED BY
ELSEVIER
CrossMark
Available online at www.sciencedirect.com
ScienceDirect
Defence Technology 11 (2015) 362−369
Defence Technology
www.elsevier.com/locate/dt

Microstructure, mechanical and corrosion behavior of high strength AA7075 aluminium alloy friction stir welds − Effect of post weld heat treatment

P. Vijaya Kumar [a], G. Madhusudhan Reddy [b], K. Srinivasa Rao [c,*]

[a] Department of Mechanical Engineering, R.I.T., Visakhapatnam, India
[b] Defence Metallurgical Research Laboratory, Hyderabad, India
[c] Department of Metallurgical Engineering, Andhra University, Visakhapatnam, India

Received 18 March 2015; revised 21 April 2015; accepted 22 April 2015
Available online 27 May 2015

Abstract

High strength aluminium alloy AA7075 (Al−Zn−Mg−Cu) is a precipitate hardenable alloy widely used in the aerospace, defense, marine and automobile industries. Use of the heat treatable aluminium alloys in all these sectors is ever-increasing owing to their excellent strength-to-weight ratio and reasonably good corrosion resistance. The shortage in corrosion resistance, however, usually poses negative concern about their reliability and lifetime when they service in the variable marine environments. These alloys also exhibit low weldability due to poor solidification microstructure, porosity in fusion zone and lose their mechanical properties when they are welded by fusion welding techniques. Friction stir welding (FSW) is a reliable technique to retain the properties of the alloy as the joining takes place in the solid state. The welds are susceptible to corrosion due to the microstructural changes in the weld nugget during FSW. In this work, the effect of post weld treatments, viz., peak aging (T6) and retrogression & reaging (RRA), on the microstructure, mechanical properties and pitting corrosion has been studied. Friction stir welding of 8 mm-thick AA7075 alloy was carried out. The microstructural changes of base metal and nugget zone of friction stir welds were studied using optical microscopy, scanning electron microscopy and transmission electron microscopy. Tensile and hardness test of base metal and welds has been carried out. Pitting corrosion resistance was determined through dynamic polarization test.

It was observed that the hardness and strength of weld were observed to be comparatively high in peak aged (T6) condition but the welds showed poor corrosion resistance. The resistance to pitting corrosion was improved and the mechanical properties were maintained by RRA treatment. The resistance to pitting corrosion was improved in RRA condition with the minimum loss of weld strength.

Keywords: FSW; AA7075; Post weld heat treatment; Pitting corrosion; Hardness

1. Introduction

Even though the mechanical properties of aluminium alloys are better, their poor corrosion resistance, particularly in welded condition limits their application range. Much attention has been dedicated to the corrosion behavior of AA7075 alloy since this material is extensively used in aerospace, defense and military applications due to its good mechanical performance and low density. AA7075 aluminium alloy is a precipitation hardening alloy containing zinc (5.1−6.1 wt.%), magnesium (2.1−2.9 wt.%) and copper (1.2−2.0 wt.%) as its main alloying elements.

Fusion welding of AA7075 alloy is difficult due to solidification and liquation cracking. Friction stir welding (FSW) is an energy efficient, environment-friendly solid state welding process. Because of the absence of parent metal melting and related problems, such as brittle dendrite structure, porosity, distortion and residual stresses, this process can be used for joining most of the aluminium alloys [1]. FSW of aluminium

* Corresponding author.
E-mail addresses: vijayakumarrit@gmail.com (P.V. KUMAR), gmreddy_dmrl@yahoo.com (G.M. REDDY), arunaraok@yahoo.com (K.S. RAO).
Peer review under responsibility of China Ordnance Society.

http://dx.doi.org/10.1016/j.dt.2015.04.003

alloys offers the advantages of low heat input, reduced distortion, low residual stress and higher mechanical property compared to the conventional fusion welding methods [2].

During FSW the material is subjected to an intense plastic deformation at elevated temperatures due to the stirring action of a rotating tool [3]. Friction stir welding achieves solid phase joining by locally introducing the frictional heat and plastic flow by rotation of the welding tool with resulting local microstructure change in aluminium alloys [6]. The welding temperature in friction stir welding of AA7075 alloys ranges between 425 °C and 480 °C. The friction stir welded joint is divided into four zones: base metal (BM), heat affected zone (HAZ), thermo-mechanically affected zone (TMAZ) and nugget zone (NZ). The welding temperature never exceeds 80% of the melting point temperature of the base alloy and does not cause melting. But the temperature is high enough to cause the dissolution/overaging of strengthening particles in HAZ, TMAZ and NZ, leading to the formation of a softened region with degraded mechanical properties generally in heat affected zone [5,7]. FSW causes grain refinement in the weld zone due to which the tensile strength of the joint increases with little loss of ductility [4].

It was reported that the microstructure in HAZ, TMAZ and WN vary particularly in precipitation hardenable aluminium alloys like 7xxx series [7]. The variation in microstructure leads to the variation in hardness and corrosion resistance of AA7075 aluminium weld. The softening of HAZ is one of the reasons why the corrosion resistance of AA7075 aluminium weld is poor. As the FSW process induces a dramatic change in microstructures, there is every need to understand the microstructure and corrosion behavior of friction stir welds [7].

Several methods are being considered for minimizing the softening and improving the properties of FSW weld joints, such as optimization of process parameters, post weld heat treatment, in process cooling using external coolants, and underwater or submerged FSW. Many authors reported that the post weld heat treatment of AA7075 alloys at overaged (T73) temper is used to improve the corrosion resistance. However, there is a loss of strength about 10%–15% compared to T6 temper. RRA treatment is used to recover the strength of 7xxx series alloys without impairing the corrosion resistance of the material. Post weld treatment to RRA leads to the dissolution of the less stable precipitates (GP zones and η') inside the grains and the increase of grain boundary precipitates. It also enhances the re-precipitation of η' ($MgZn_2$) precipitates [9–12].

From the above literature survey, the post weld heat treatments, viz. overaging (T7), peak aging (T6), and RRA are in use for improving the mechanical properties and corrosion resistance of friction stir welds of high strength AA7075 aluminium alloy. However, out of all the post weld heat treatments, the post weld heat treatment to peak aged (T6) condition gives higher strength to the joints over other available treatments. But the T6 treated welds are prone to corrosion. The corrosion resistance of friction stir welds which are post weld heat treated to RRA condition is better than other post weld heat treatment conditions without considerable loss of strength. Hence, the post weld heat treatments of T6 and RRA were selected to study the microstructure, mechanical properties and pitting corrosion resistance.

The present investigation was undertaken to determine the effects of T6 and RRA post weld heat treatment on microstructure, hardness, tensile strength and resistance to pitting corrosion of the friction stir welds of AA7075-T7 aluminium alloy.

2. Experimental details

2.1. Materials and heat treatment

The AA7075 aluminium alloy plate was friction stir welded using optimum welding process parameters. The process parameters used for the welding are given in Table 1. The dimensions of the rolled AA7075 plate are 240 mm × 150 mm × 8 mm. The chemical composition of base metal is given in Table 2. The samples for metallography, hardness measurement, tensile test and corrosion study were extracted from the welded plates. All the samples are heat treated to peak aging (T6) and RRA conditions given in Table 3.

Peak aged treatment (T6) is a solution treatment applied to aluminium alloys as per the standards ASTM B807/B807M. The RRA process was first developed by Cina and Gan [13,14] in the mid-1970s and was further developed by Oliveira et al. [15] at the National Research Council of Canada (NRC). T6 and RRA treatments are applied to the AA7075 aluminium base alloy and the friction stir welds.

Optical microscopy (OM) has been performed on the heat treated samples as per ASTM-E3 (95). The microstructures were recorded with image analyzer. Scanning electron microscopy (SEM) analysis was carried out on the samples to study the grain structure and precipitates as per ASTM-E340. The hardness of the samples is measured by using Vickers hardness tester with 0.5 kgf of load and 15 s of dwelling time (ASTM-E384). Tensile tests were conducted as per ASTM-E8/E8M on the prepared samples after the heat treatment.

A software-based potentio-dynamic polarization test was performed on the post weld treated samples of the friction stir welds as well as the heat treated base metal in order to study the effect of post weld heat treatments on pitting corrosion behavior of the alloy. A saturated calomel electrode (SCE) and a carbon electrode were used as reference and auxiliary electrodes, respectively. All experiments were conducted in aerated 3.5% NaCl solutions with PH adjusted to 10 by adding potassium hydroxide. The potential scan was carried out at 0.166 Mv/s with the initial potential of −0.25 V (OC) SCE to the final pitting potential. The exposure area for these experiments was 1 cm^2. Pitting corrosion testing has been done as per ASTM-G34. The potential at which current increased drastically was considered to be the critical pitting potential, E_{pit}. The samples exhibiting relatively more passive potentials (or less negative potentials) were considered to have better pitting corrosion resistance. Optical microscopy on

Table 1
Process parameters of friction stir welding.

Process parameters	Spindle speed/rpm	Tool down feed/(mm·min^{-1})	Depth/mm	Initial heat time/s	Tool axial feed/(mm·min^{-1})	Tool longitudinal travel/mm
Values	750	40	7.25	3	25	240

Table 2
Chemical compositions (wt.%) of 7075 aluminium alloy.

Element	Zn	Mg	Cu	Fe	Si	Ti	Mn	Cr	Al	Other
Wt.%	5.6	2.5	1.5	0.5	0.4	0.2	0.3	0.25	87.1−91.4	0.15

dynamically polarized samples was carried out to understand the mechanism of pitting.

3. Results and discussions

3.1. Microstructures of as-welded and post weld heat treated AA7075-T7 friction stir welds

Fig. 1 represents the optical micrographs of grain structure developed in the base AA7075 aluminium alloy and clearly reveals the elongated pancake shaped grains. The TEM micrographs of AA7075 aluminium alloy in different tempers are given in Fig. 2. Grain boundary precipitates ($MgZn_2$) are observed in all three conditions with different morphology. In T6 condition, the microstructure has relatively coarse and closely spaced precipitates along the grain boundaries and fine precipitates in the grains. On the other hand, in RRA condition, the grain boundary precipitates are discontinuous and coarser than that in T6 condition due to the formation of additional grain boundary precipitates during the initial phase of retrogression. The optical micrographs of nugget zone are given in Fig. 3. Fine and equiaxed recrystallized grain structure in the nugget was developed due to tool stirring action and temperature. The grain structure shows the finer grains compared to the base metal. The microstructure reveals the grains with the presence of some intermetallics. These intermetallics have been previously identified as mainly Al_7Cu_2Fe, $(Al, Cu)_6(Fe, Cu)$, and Mg_2Si. The characteristic microstructural constituents formed following T6 temper consist of GP zones, semi-coherent η ($MgZn_2$), and incoherent η ($MgZn_2$) precipitates. The high strength of T6 microstructure is mainly due to GP zones and η' precipitates, but the contribution of η' precipitates to the strength was reported to be higher. If the treatment in T6 is followed by second heating of the specimens and subsequent water quenching, the segregations are formed in the order, GP zones $\rightarrow \eta' \rightarrow \eta$ SEM micrographs of weld nugget in As-welded, PWHT- T6 and PWHT- RRA are given in Fig. 4).

The as-received material has a grain size of 50−60 μm where as the nugget zone has a grain size of 6−14 μm. The grain size in TMAZ is random and the grain size varied between 20 and 30 μm. The HAZ is not affected by the tool action but the grain size is closer to the parent metal grain size of 50 μm. The sizes of η and η' precipitates in as-received AA7075-T7 aluminium alloy vary from 50 nm to 100 nm. The weld nugget has finer η and η' precipitates with size of 10−30 nm. The coarsened η and η' precipitates with size of 50−150 nm were found in HAZ. The sizes of η and η' precipitates in TMAZ were 100 nm [9].

EDAX results of weld samples in post weld heat treated (PWHT) conditions of T6 and RRA are shown in Fig. 5(a) and

Table 3
Heat treatment procedures for alloy investigation.

	Temper condition	Aging temperature
T6	Near peak aging	Solution heat treatment at 515 °C for 1.5 h with cold water quench and heating at 120 °C for 24 h.
Retrogression and reaging (RRA)	Peak aging	Heat treatment at 220 °C for 5 min and then water quenching followed by aging at T6 condition.

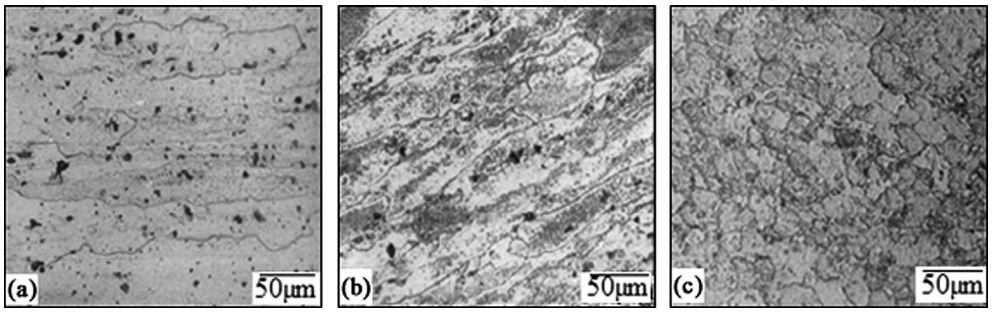

Fig. 1. Optical micrographs of AA7075 alloy base metal (a) As-received (b) T6 (c) RRA.

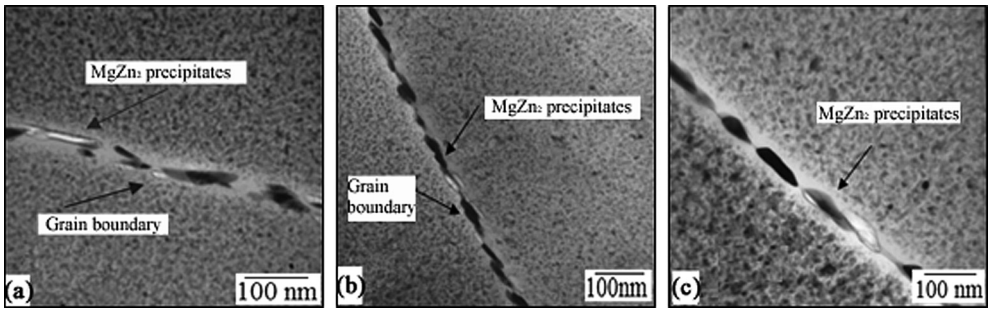

Fig. 2. TEM photographs of AA7075 alloy base metal (a) As-received (b) T6 (c) RRA.

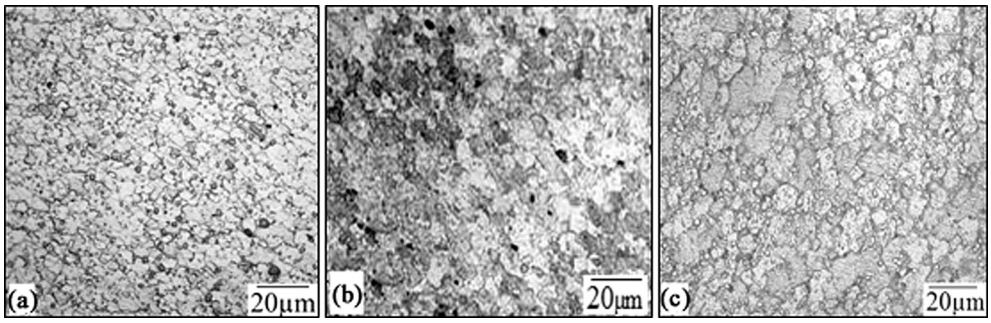

Fig. 3. Optical micrographs of nugget zone: (a) As-welded (b) PWHTT6 (c) PWHT RRA.

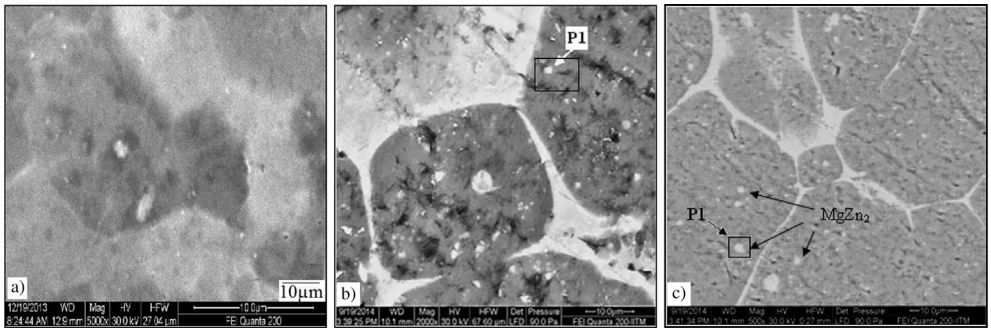

Fig. 4. SEM images of weld nugget in different temper conditions: a) As-welded, b) T6, and c) Retrogression & Re-aging (RRA).

(b). Evidence of Mg–Zn precipitates can be seen from the EDAX results.

3.2. Hardness measurements

The hardness values measured at various points from the weld centre are presented in Table 4. From the results it is observed that the variation of hardness is greatly influenced by the post weld heat treatment processes. The hardness profiles of the welded joints in different heat treated conditions are presented in Fig. 6. The average value of base metal hardness is 150 H_V. The hardness measurements were taken at 2 mm below the weld surfaces of the plates. The average hardness values in the weld nugget (WN) zone and the heat affected zone (HAZ) are 158 Hv and 160 Hv, respectively. The standard deviation and variance in hardness measurements were 1.649 and 2.72, respectively. These are less than the hardness of base metal (BM). It was observed that the hardness is high in T6 condition compared to other post weld heat treatments.

The overaging and dissolving of the metastable precipitates lead to the decrease in the hardness in WN. But the presence of the fine equiaxed grains and the resolution of the dissolved precipitates partially remedy the loss of hardness. The improved hardness in WN is attributed to the recovery of the dissolved precipitates and the fine equiaxed grains in WN. Friction stir welding generates a region of relatively low hardness value around weld centre.

This region extends up to the transition zone of TMAZ and HAZ. The HAZ region showed a decrease in hardness arising from the coarsening of the precipitates in this region. The dissolution of strengthening precipitates ($MgZn_2$) in HAZ may be attributed to the reduction in hardness.

3.3. Tensile tests

The Tensile properties of the FSW joints are dependent on the microstructure which in turn depends on the welding conditions, base metal initial temper conditions and post weld treatments. The stress–strain curves of base alloy and weld

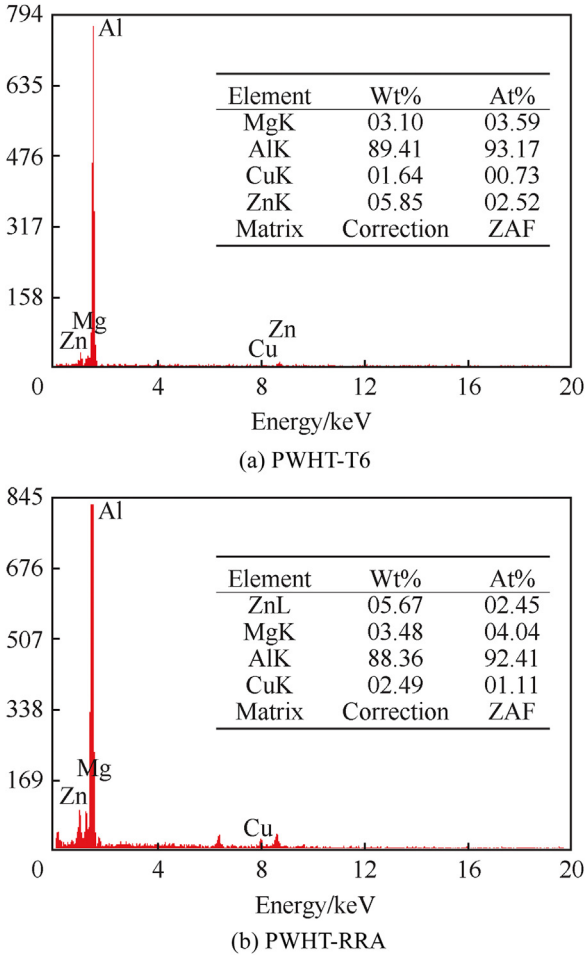

Fig. 5. a) & b) EDAX result of friction stir welds in PWHT -T6 and PWHT - RRA

Table 4
Hardness values in various zones of welds in different temper conditions.

	BM	HAZ	TMAZ	Nugget			TMAZ	HAZ	BM
Distance from weld centre/mm	−20	−15	−10	−5	0	5	10	15	20
As-welded	143	141	156	146	145	147	157	142	143
T6	165	154	164	157	158	158	165	155	165
RRA	160	152	161	156	155	157	162	153	160

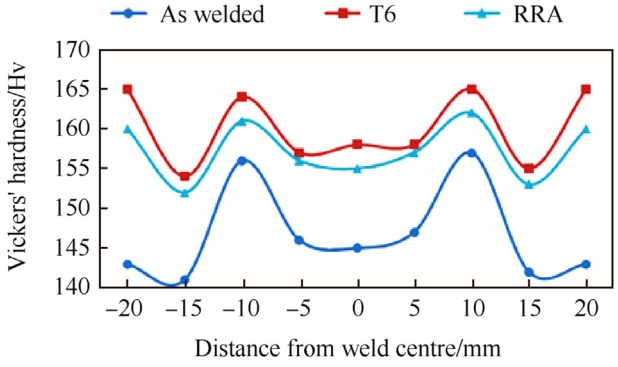

Fig. 6. Hardness measurements in various zones of welds in different temper conditions.

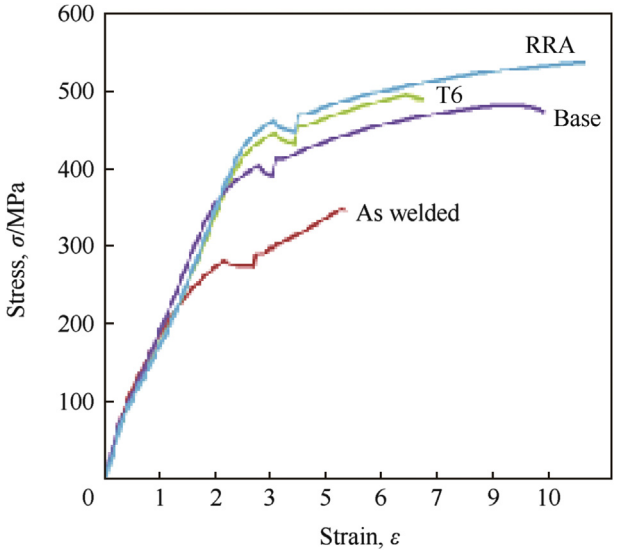

Fig. 7. Stress-strain diagram of base alloy and welded specimens in different post weld heat treated conditions.

Table 5
Tensile properties of base alloy and welded specimens in different post weld heat treated conditions.

No.	Sample temper condition	Y.S./MPa	UTS/MPa	Elongation/%
1	Base metal	421	482	8.4
2	As welded	227	346	4.6
3	T6	452	540	10.4
4	RRA	420	553	11

samples in different post weld heat treated conditions are shown in Fig. 7. The tensile properties of the joints in post weld heat treated and as-welded conditions are summarized in Table 5 and Fig. 8. The standard deviation and variance in tensile testing measurements were 3.6 and 12.96, respectively.

It is evident from the above results that the post weld heat treatments significantly influence the tensile properties of FSW joints. The RRA treatment improved the tensile properties of the FSW joint compared to the as-welded condition. The yield strength (Y.S.), ultimate tensile strength (UTS) and % elongation of FSW joints in RRA treatment are increased

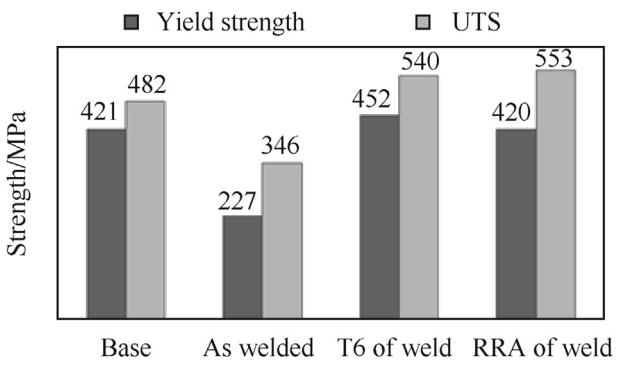

Fig. 8. Tensile properties of friction stir welds in different post weld heat treated conditions.

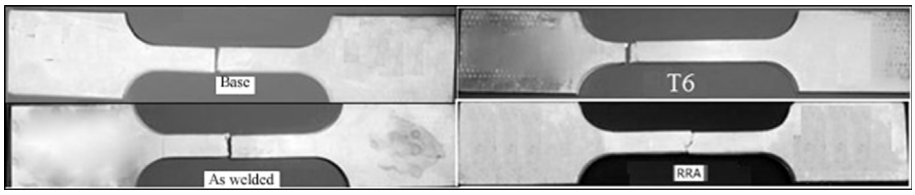

Fig. 9. Fracture locations of tensile samples of welds in different temper conditions.

by 45%, 35%, and 48%, respectively, compared to those in the as-welded condition. The strength and elongation of the joints were also improved in T6, and RRA conditions.

The very fine precipitates of GP zones are distributed homogeneously inside the coarser grains, and the less spaced η' grain boundary precipitates can be observed in T6 temper condition. The presence of fine precipitate structure of GP zones and metastable phase η' are attributable to the strengthening of alloy. The majority of the precipitates are of η' type and more stable GP-II zones are present in smaller amount [8]. The base metal (T7) sample contains the coarser precipitates which uniformly distribute inside the grains. The precipitates in T7 samples are essentially η precipitates with few η' precipitates.

3.4. Fractography

The location of fracture on the tensile samples is shown in Fig. 9. The SEM analysis was performed on the fractured tensile samples of friction stir welded AA7075 alloy and is shown in Fig. 10. SEM fracture surface micrographs show the deep grooves on the specimen edges where the elongated grains pulled out when de-cohesion occurred in the grain boundaries.

The fractures in two conditions are all in transgranular/intergranular combined mode. And both the conditions represent fibrous ductile fracture, with many small dimples being inside the surface of fibrous fracture. There are more transcrystalline fractures and fewer intergranular fractures caused by the second phases within the dimples. The fracture behavior of alloy is due to the reduction of undissolved coarser phase and the increase of precipitated phase (the increase of yield strength).

3.5. Pitting corrosion

Determining the density of current in aluminium alloy is difficult since the aluminium can be easily passivated through

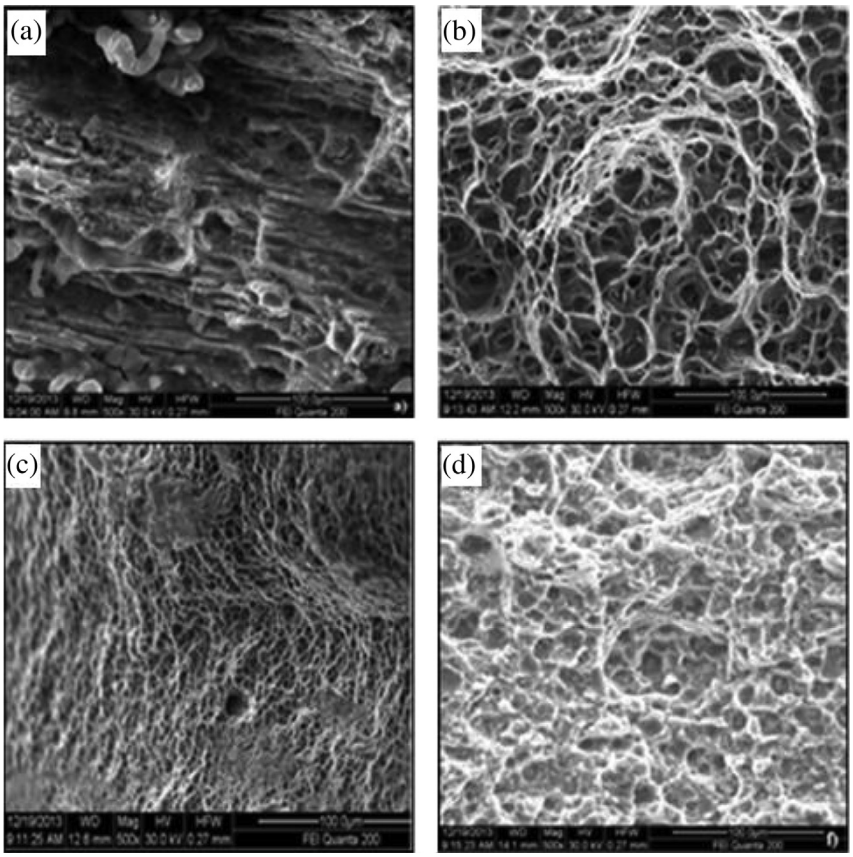

Fig. 10. SEM Fractographs of fractured tensile samples of welds in various temper conditions. (a) Base, (b) As-welded, (c) T6, (d) RRA.

Table 6
Pitting potential values of AA7075 base metal and friction stir welds in various zones in different post weld conditions.

	Pitting potential values/mV		
	As-received	T6	RRA
Base	−740	−840	−491
Weld zone	As-welded	T6	RRA
Nugget	−755	−781	−590
TMAZ	−794	−678	−635
HAZ	−738	−706	−569

the growth of a protective film, making more difficult or impeding the measurements of the current densities. One way to overcome this difficulty is to activate the samples by means of a cathodic polarization and to perform sweep up to the anodic potentials at relatively high rate. This method provides a determination of the anodic curve under relatively film-free conditions. The pitting potential values at various regions of welds in T6 and RRA post weld treatment conditions are presented in Table 6. After T6 treatment, the TMAZ has more resistance to pitting compared to other regions. The TMAZ has showed the improved corrosion resistance in the heat treatment order: as-welded, T6 and RRA. The same order of improvement was observed in the other regions, i.e., BM, Nugget and HAZ. The HAZ is less resistant to pitting compared to other regions. Higher pitting potential was observe in the weld nugget in RRA condition. The potentiodynamic polarization curves for various weld regions along with the pitting potential values are shown in Fig. 11(a)–(d).

The pitting corrosion was mainly attributed to the difference in potential between the matrix and grain boundary precipitates and influenced by a range of the microstructural features, such as size and interspaces of precipitates, precipitation free zones and solute concentration gradients.

The RRA sample showed more resistance to pitting compared to that of as-welded and peak ages samples. From Table 6 it is evident that there is a significant improvement of corrosion resistance in nugget and TMAZ regions after RRA treatment. Hence the post weld heat treatments have an obvious impact on the electrochemical response.

The coarsened grains in the weld regions are distributed uniformly and gain the original fine grain geometries after RRA treatment, and the weld region regained a homogenous structure. After the RRA treatment, the increased concentration copper alloy content in the precipitate's composition may have led to the improved resistance to pitting corrosion. The presence of Mg and Zn in the precipitates promotes the susceptibility to pitting corrosion.

The microstructure of AA7075-T7 shows the grain boundary precipitates that are much coarser than those in the T6 temper. The RRA treatment leads to a combination of grain boundary precipitate coarsening, which resembles the precipitates formed in the T7 temper, and the precipitate distribution in the matrix resembles the precipitates formed in the T6 temper. This combination results in good performance with respect to both the mechanical strength and the resistance to corrosion.

RRA treatment had shown more corrosion resistance than peak aging condition (T6). Poor corrosion resistance in T6

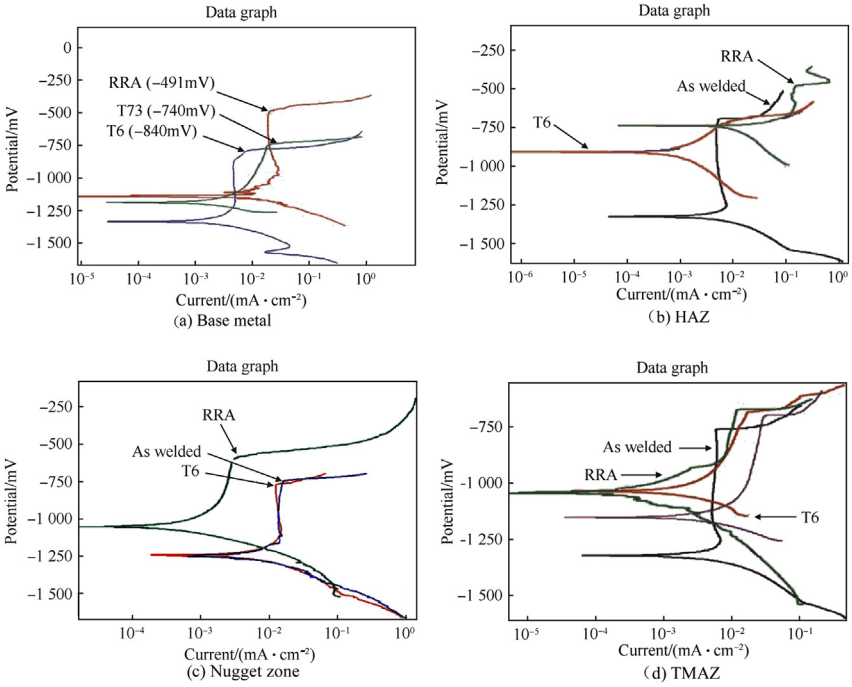

Fig. 11. Potentiodynamic polarization curves of AA7075 alloy.

condition may be due to the precipitates of Zn and Mg and less amount of copper in the precipitates.

4. Conclusions

1) Microstructure in T6 condition has the relatively coarse and closely spaced precipitates along the grain boundaries and the fine precipitates within the grains. On the other hand, in RRA condition, the grain boundary precipitates are discontinuous and coarser than that in T6 condition due to the formation of additional grain boundary precipitates during the initial phase of retrogression.
2) Reduced hardness in the WN is attributed to the dissolution of the less stable phases (GP and η') and the decrease in dislocation density. The improved hardness in TMAZ is due to the formation and growth of η' phase segregations to a specific size during RRA treatment. Coarsening and dissolution of η' phases reduced the hardness in HAZ.
3) RRA promotes coarse precipitation of the equilibrium phase η in the grains and sub-grain boundaries, while maintaining a fine distribution of η' in the grain interiors. The increased strength and hardness in the peak aging (T6) condition were attributed to the presence of semi-coherent intermediate η' ($MgZn_2$). There was an improvement in the tensile strength of RRA sample close to the strength of T6 sample.
4) Due to the discontinuous grain boundary precipitates with large spacing, no continuous chain exists for corrosion to take place. As a result, their susceptibility to pitting corrosion is reduced in the RRA samples. The finer grains and continuous precipitates along the grain boundaries in T6 samples lead to high pitting corrosion.
5) Post weld heat treatment of AA7075 alloy friction stir weld to Retrogression and reaging (RRA) treatment had shown a good combination of high tensile strength and corrosion resistance over as-welded and PWHT-T6 samples.

Acknowledgements

The authors would like to thank Dr. A.Ghokale, Director, Defence Metallurgical Research Laboratory, Hyderabad, India for his continued encouragement and permission to publish this work.

References

[1] Sharma Chaitanya, Dwivedi Dheerendra Kumar, Kumar Pradeep. Effect of welding parameters on microstructure and mechanical properties of friction stir welded joints of AA7039 aluminum alloy. Mater Des 2012:379−90.
[2] Szklarska-Smialowska Z. Pitting corrosion of aluminum. Corros Sci 1999;41:1743−67.
[3] T. Azimzadegan, Gh. Khalaj, M.M. Kaykha, A.R. Heidari, Ageing behavior of friction stir welding AA7075-T6 aluminum alloy, Comput Eng Syst Appl. (Volume II): 183-187.
[4] Paglia CS, Buchheit RG. A look in the corrosion of aluminum alloy friction stir welds. Scr Mater 2008;58:383−7.
[5] Karaaslan A, Kaya I, Atapek H. Effect of aging temperature and of retrogression treatment time on the microstructure and mechanical properties of alloy AA 7075. Metal Sci Heat Treat 2007;49:9−10.
[6] Venugopal T, Srinivasa Rao K, Prasad Rao K. Studies on friction stir welded AA7075 aluminum alloy. Trans Indian Inst Metals December 2004;57(6):659−63.
[7] Rao K Srinivasa, Rao K Prasad. Pitting corrosion of heat-treatable aluminium alloys and welds: a review. Trans Indian Inst Met December 2004;57(No. 6):593−610.
[8] Ranganatha R. Multi-stage heat treatment of aluminum alloy AA7049. Trans Nonferrous Met Soc China 2013:1570−5.
[9] Su JQ. Microstructural investigation of friction stir welded 7050- T651 aluminium. Acta Mater 2003;51:713−29.
[10] Hassan KhAA, Norma AF, Price DA, Prangnell PB. Stability of nugget zone grain structures in high strength Al-alloy friction stir welds during solution treatment. Acta Mater 2003;51(7):1923−36.
[11] Sullivan A, Robson JD. Microstructural properties of friction stir welded and post weld heated 7449 aluminum alloy thick plate. Mater Sci Eng A 2008;478:351−60.
[12] Feng JC, Chen YC, Liu HJ. Effect of post weld heat treatment on microstructure and mechanical properties of friction stir welded joints of 2219-O aluminum alloy. Mater Sci Technol 2006;22(1):86−90.
[13] Cina B and Gan R. Reducing the susceptibility of alloys, particularly aluminum alloys, to stress corrosion cracking. United States Patent 3856584; 24 December 1974.
[14] Cina B, Zeidess F. Advances in the heat treatment of 7000 type aluminum alloys by retrogression and re-aging. Mater Sci Forum 1992;102−104.
[15] Oliveira Jr AF, de Barros MC, Cardoso KR, Travessa DN. The effect of RRA on the strength and SCC resistance on AA7050 and AA7150 aluminum alloys. Mater Sci Eng 2004;379A:321−6.